

Targeting firing rate neuronal homeostasis can prevent seizures

Fred Mulroe^{1,§}, Wei-Hsiang Lin^{1,§}, Connie Mackenzie-Gray Scott², Najat Aourz³,
Yuen Ngan Fan^{1,*}, Graham Coutts^{1,4}, R. Ryley Parrish^{2,‡}, Ilse Smolders³, Andrew Trevelyan²,
Robert Wykes⁵, Stuart Allan^{1,4}, Sally Freeman⁵ and Richard A. Baines^{1,¶}

¹Division of Neuroscience and Experimental Psychology, School of Biological Sciences, Faculty of Biology, Medicine and Health, University of Manchester, Manchester Academic Health Science Centre, Manchester, UK

²Institute of Neuroscience, University of Newcastle, UK

³Department of Pharmaceutical Chemistry, Drug Analysis and Drug Information, Research group Experimental Pharmacology, Center for Neurosciences, Vrije Universiteit Brussel, Brussels, Belgium

⁴Geoffrey Jefferson Brain Research Centre, The Manchester Academic Health Science Centre, Northern Care Alliance NHS Foundation Trust, University of Manchester, UK

⁵Division of Pharmacy & Optometry, School of Health Sciences, Faculty of Biology, Medicine and Health, University of Manchester, Manchester Academic Health Science Centre, Manchester, UK

*Present address: Imagen, Enterprise House, Lloyd Street North, Manchester M15 6SE, UK.

‡Present address: Department of Cellular and Molecular Biology, Xenon Pharmaceuticals, Burnaby, BC, Canada.

§These authors contributed equally to this work

¶Author for correspondence (Richard.Baines@manchester.ac.uk)

Abstract

Manipulating firing-rate neuronal homeostasis, which enables neurons to regulate their intrinsic excitability, offers an attractive opportunity to prevent seizures. However, to date, no drug-based interventions have been reported that manipulate this type of neuronal homeostatic mechanism. Here, we use a combination of *Drosophila* and mouse and, in the latter, both a pentylentetrazole (PTZ) induced seizure model, and an electrically induced seizure model for refractory seizures to evaluate anticonvulsant efficacy of a novel class of anticonvulsant compounds, based on 4-*tert*-butyl-benzaldehyde (4-TBB). The mode-of-action includes increased expression of the firing rate homeostatic regulator PUMILIO (PUM). Knock-down of *PUM* expression, in *Drosophila*, blocks anticonvulsive effects of 4-TBB, whilst analysis of validated PUM targets in mouse brain show significant reductions following exposure to this compound. A structure-activity study identifies the active parts of the molecule and, further, shows the pyrazole analogue demonstrates highest efficacy,

being active against both PTZ-, and electrically-induced, seizures. This study provides a proof-of-principle that anticonvulsant effects can be achieved through regulation of firing rate neuronal homeostasis and identifies a possible chemical compound for future development.

Summary

Epilepsy remains challenging to treat. In this study, we show that manipulating endogenous mechanisms that maintain stability of neuronal activity, represent a possible route to better manage this disorder.

KEY WORDS: *Drosophila*, Seizure, Neuronal homeostasis, Mouse, PUMILIO, Translational regulation

Introduction

Firing rate neuronal homeostasis provides a possible target to achieve therapeutic control of epilepsy. This is because such neuronal homeostatic mechanisms ostensibly oppose extremes of neuronal activity that are normally associated with seizures. By maintaining neuronal activity patterns at physiologically relevant ‘set-points’, neuronal homeostasis maintains stability of both neuron and network function across the life-course (Giachello and Baines, 2017). However, to date, neuronal homeostasis, of any kind, has not been specifically targeted for clinical benefit.

PUMILIO (PUM) homeostatically maintains action potential firing rates within a set-range (Driscoll et al., 2013). A translational repressor, PUM binds mRNA transcripts and reduces *de novo* protein synthesis, with increased *PUM* expression occurring in *Drosophila* neurons exposed to increased synaptic excitation. Conversely, as synaptic excitations fall, *PUM* expression is reduced (Mee et al., 2004). The 3'-UTR of PUM-regulated transcripts usually contain one or more copies of a PUM-Response Element (PRE: UGUANAUA, where N is A, C, G or U) (Gerber et al., 2006). Analysis of both *Drosophila* and mammalian transcriptomes identifies greater than 1000 transcripts that contain one or more PREs, consistent with a broad regulatory role (Zhang et al., 2017). Many of these transcripts are shared across the two animal species indicative of common regulation by PUM (Bohn et al., 2018; Gerber et al., 2006). However, PUM function as a homeostatic regulator requires additional co-factors (including Nanos and Brain-tumor), that may be tissue-specific. Thus, the actual effect of PUM, in any species, is likely dictated by presence of co-factors and both the number and proximity of additional co-factor binding elements, in addition to the number of PREs (Arvola et al., 2017; Muraro et al., 2008). In mammals, PUM-regulated transcripts that have

potential to influence neuron activity include $\text{Na}_v1.6$ (SCN8A) (Driscoll et al., 2013) and GLUR2 (AMPA receptor) (Dong et al., 2018). PUM-dependent homeostatic translational repression of $\text{Na}_v1.6$, in rat cortical pyramidal neurons, reduces the amplitude of expressed voltage-gated Na^+ current (I_{Na}) and lowers action potential firing frequency (Driscoll et al., 2013). Down-regulation of AMPA receptor expression may also be expected to be anticonvulsant, evidenced by the anti-epileptic compound, perampanel, which is an allosteric antagonist of AMPA receptors (Patsalos, 2015).

Whilst *Drosophila* has one *PUM* gene, mammals express two highly similar orthologues (*PUM 1* & *2*) that are co-expressed, and which bind identical RNA motifs and, thus, appear to act redundantly (Bohn et al., 2018; Galgano et al., 2008; Hogan et al., 2015). Seizure occurrence could reflect reduced homeostatic capability and it is significant that recent studies suggest reduced PUM contributes to epilepsy. Specifically, i) *PUM 1* or *2* haploinsufficiency is associated with spontaneous seizures in mice (Follwaczny et al., 2017; Gennarino et al., 2015; Siemen et al., 2011), ii) *PUM2* expression is reduced in human patients suffering temporal lobe epilepsy and in rat hippocampus following pilocarpine-induced seizure (Wu et al., 2015), and iii) *PUM* expression is reduced in *Drosophila* genetic seizure mutations (Lin et al., 2017). In the latter, transgenic up-regulation of *PUM* is potentially anticonvulsant in these same *Drosophila* mutations (Lin et al., 2017).

Based on a screen to identify chemicals that increase expression and/or stability of PUM, we identified avobenzonone, which secondary screens show is anticonvulsant in seizure-sensitive *Drosophila* (Lin et al., 2017). However, the physiochemical properties of avobenzonone are not compatible with clinical use. Thus, in this study, we report the identification of an avobenzonone analogue, 4-*tert*-butyl-benzaldehyde (4-TBB), that is anticonvulsant and has properties (e.g. solubility) more consistent with clinically active compounds. We show that 4-TBB and analogues (specifically the pyrazole RAB216) are active against a range of *Drosophila* seizure mutants and, significantly, reduce severity of both pentylenetetrazol (PTZ)- and pharmacoresistant electrically (6Hz)-induced seizures in mouse. Reduction of seizure, in fly and mouse, is accompanied by increased expression of PUM. We further report down-regulation of known PUM targets following exposure of mouse brain to 4-TBB thus validating proposed mode-of-action. Thus, this study provides a proof-of-principle that firing rate neuronal homeostasis can be manipulated for possible anticonvulsant therapy. However, we cannot currently state that 4-TBB (and analogues) only increases PUM expression, which would require full mode-of-action studies.

Results

4-TBB suppresses seizure behaviour in *Drosophila*

Single *Drosophila* gene mutations increase seizure-like activity in response to electric-shock (Baines et al., 2017). In a prior study, we identified avobenzonone to both increase *PUM* expression and reduce seizure severity in such *Drosophila* mutations (Lin et al., 2017). Avobenzonone is, however, poorly water soluble and therefore we identified a breakdown product, 4-TBB to be a better candidate for analysis of mode-of-action. We tested the anticonvulsant activity of 4-TBB in three diverse seizure mutants to demonstrate wide applicability, regardless of the underlying genetic cause of seizure. Exposure to drug (1.2 mM contained within food, dose available to the CNS is unknown) was sufficient to reduce electroshock-induced seizure duration in *bangsenseless¹* (*para^{bss}*; Na_v hypermorph, 194 ± 116 vs. 348 ± 101 s, 4-TBB vs. control, $n = 30$, $p < 0.001$), *easilyshocked* (*eam*; ethanolamine kinase deficiency, 160 ± 81 vs. 232 ± 124 s, $n = 30$, $p = 0.011$) and *julius seizure* (*jus*; a transmembrane domain protein of undetermined function, 197 ± 124 vs. 266 ± 112 s, $n = 30$, $p = 0.03$, Fig. 1A). The level of seizure suppression observed for 4-TBB, in all mutations, compared favourably to an equal dose of the established anticonvulsant phenytoin (PHE, *c.f.* Fig. 1D), perhaps indicative of equal potency assuming similar pharmacokinetics.

The expression of *PUM* is reduced in *para^{bss}* mutants and, moreover, increasing *PUM* expression in this mutant background is sufficient to suppress seizure activity in response to electroshock (Lin et al., 2017). To determine whether the anticonvulsant effect of 4-TBB is associated with up-regulation of *PUM*, we used a *PUM*-minimal promoter construct upstream of GAL4 (*dpum*-GAL4) to drive expression of UAS-luciferase (UAS-luc) (Lin and Baines, 2019). Exposure of *dpum*-GAL4>UAS-Luc flies to 4-TBB (1.2 mM in flyfood) resulted in a significant increase in luciferase activity (2.7 ± 1.5 fold change, $n = 5$, $p = 0.03$, vehicle control set as 1) (Fig. 1B). We adopted this approach because available anti-PUM antibodies (designed to rodent PUM 1 and 2) do not work well in *Drosophila*. We also observed a significant increase in *PUM* transcript abundance, measured by QRT-PCR, of ~60% (1.6 ± 0.3 fold change, $n = 5$, $p = 0.002$, vehicle control set as 1) following exposure to the same amount of 4-TBB (Fig. 1C). Finally, we find that the anticonvulsive activity of 4-TBB is significantly diminished when *PUM* expression is reduced in the CNS, via targeted expression of an RNAi construct (Fig. 1D). PHE, which has a different mode of action (Yaari et al., 1986), remains active under these conditions. We conclude that the mode-of-action of 4-TBB requires the presence of PUM and increases expression of this homeostatic regulator.

4-TBB reduces epileptiform activity in mouse hippocampal culture slices

Incubation of acutely-harvested mouse brain slice with 4-TBB (1.2mM in the bathing media) for 2h was sufficient to produce a significant increase in PUM2 expression (PUM1 not measured), as determined by Western Blot (2.5 ± 0.3 fold compared to vehicle-treated controls which were the corresponding slice taken from the opposite hemisphere incubated in vehicle only, $n = 5$, $p = 0.003$, Fig. 2A). Addition of a similar amount of 4-TBB (1.2mM) to mouse organotypic hippocampal slices, in which epileptiform activity was already established (Fig. 2B-C), led to a progressive reduction in epileptiform activity ($p < 0.0001$; $n = 7$ and 8 , control vs. 4-TBB, respectively) compared to controls (vehicle only) that was apparent by 1h, and maximal after 3h (Fig. 2D-E). Following exposure to 4-TBB, a selection of slices were exposed to 4-aminopyridine (4-AP, 100 μm) which, as expected, rapidly induced increased activity (sFig.1). This demonstrates that slices were healthy following exposure to 4-TBB. Whilst we acknowledge that the concentration of 4-TBB used in these experiments is high, the sole purpose was to show that this compound could elicit increased PUM expression, and exhibits associated anticonvulsive effects, in rodent brain tissue, prior to testing *in vivo*.

4-TBB reduces induced PTZ-induced seizure in mice

A standard protocol for PTZ-induced seizures is to apply a test compound immediately (up to 1hr) prior to PTZ exposure (Chen et al., 2011; Erdtmann-Vourliotis et al., 1998). Our preliminary experiments showed that such dosing with 4-TBB (at a maximal dose of 800 mg/kg, s.c. injection 1hr prior) was ineffective in preventing PTZ-induced seizures. Thus, to allow longer time for drug to access the brain, mice were exposed to 4-TBB (800 mg/kg, s.c. injection) or saline vehicle (CTRL), once per day for 3 days prior to PTZ exposure (no other dosing regimens were tested). We observed no overt change in animal behaviour, nor weight loss, during the test-period. Four hours after the last injection on day 3, seizures were induced by PTZ (60 mg/kg, s.c. injection). Latency to onset of Straub tailing (a first clear indicator of seizure) was significantly delayed in the 4-TBB-exposed group (215.0 ± 81.0 vs. 138.3 ± 47.3 s, $n = 12$ and 16 , respectively, $p = 0.004$, Fig. 3A). Time to onset of first generalised tonic-clonic seizure (rearing and falling) was also significantly delayed (239 ± 59 vs. 166.8 ± 44.1 s, 4-TBB vs. saline control, $n = 12$ and 16 , respectively, $p = 0.001$, Fig. 3B). To confirm the expectation that the anticonvulsive effect of 4-TBB was associated with up-regulation of PUM, *post-mortem* brains were probed by Western blot. Expression of PUM1 and PUM2 were significantly up-regulated in 4-TBB-exposed mice (1.4 ± 0.3 and 1.2 ± 0.2 fold increase, $p < 0.0001$ and $p = 0.01$, respectively, Fig. 3C) compared to the saline controls (set as 1).

Validated PUM-dependent regulated transcripts, in mammals, include *Nav1.1* (*SCN1A*), *Nav1.6* (*SCN8A*) and *GLUR2* (aka *GLUR-A*, AMPA receptor) (Dong et al., 2018; Driscoll et al., 2013; Vessey et al., 2010). Bioinformatic analysis of expressed mRNAs also identifies a putative PRE motif in *Nav1.2* (*SCN2A*), indicative that this channel variant is also regulated by PUM (Bohn et al., 2018). Western blot (Fig. 3D) of the same brain extracts, as above, shows that the expression level of *Nav1.1*, *Nav1.2* (0.73 ± 0.2 and 0.79 ± 0.16 , $p = 0.005$ and 0.007 , respectively, $n = 14$) and *GLUR2* (0.75 ± 0.26 , $p = 0.001$, $n = 14$) were significantly reduced in brain tissue exposed to 4-TBB. No change was observed for *Nav1.6* (0.94 ± 0.12 , $p = 0.75$).

Identification of a more potent 4-TBB analogue

The above data shows clear proof-of-principle that a compound able to increase PUM expression has potential to be exploited as an anticonvulsant. However, the active concentration of 4-TBB required for significant effect, in the *in vivo* mouse PTZ-induced seizure assay (800mg/kg) is unacceptably high. Testing 4-TBB at a lower dose (400mg/kg) reduced seizure behaviour but did not result in statistically significant effects (data not shown). To identify a more potent 4-TBB analogue, that may be better suited for clinical use, we exploited *Drosophila para^{bss}* to screen for anticonvulsive activity of a diverse set of fourteen (synthesised or purchased) 4-TBB related compounds (Fig. 4A, all structures and chemical properties are shown in sTable 1). All compounds were initially tested at 2mM (concentration in flyfood, amount reaching CNS unknown). The commonly used antiepileptic, sodium valproate (VPA, 2mM) was also included as a positive control. We identified 4-(3,5-dimethyl-1*H*-pyrazol-4-yl)benzoic acid (hereafter termed RAB216) to be the most effective analogue against *para^{bss}* (Fig. 4A). This analogue was active at 0.1mM (concentration in flyfood) whilst 4-TBB and VPA were inactive at this reduced concentration (Fig. 4B).

Analysis of mouse brain exposed, *in vivo*, to RAB216 (200mg/kg, once per day for 3 days), showed a significant increase in PUM2 expression ($p = 0.01$), and a smaller (but not significant, $p = 0.07$) increase in PUM1 (Fig. 5A). As an additional control for mode-of-action, we also screened for effect of valproate (VPA, an effective anticonvulsant in the PTZ-induced seizure assay) and saw no change to either PUM1 or 2 (Fig. 5B). Consistent with its heightened potency to increase PUM2 (*c.f.* Fig. 3C), RAB216 was > 4x more active than 4-TBB in protecting mice against PTZ-induced seizures, being significantly active at 200mg/kg (Fig. 5C-D), a dose which prevented the induction of seizure in 50% of animals tested ($p = 0.05$, Fig. 5E). By contrast, a repeat of 4-TBB exposure (800mg/kg), in this assay, prevented tonic-clonic seizures (rearing and falling) in only 30% of

animals during the 20min observation period (not significantly different to CTRL, data not shown). This provides confidence that further, yet more active chemical structures, are yet to be discovered and the results we present here provide a suitable starting point for this ambition.

Finally, we tested RAB216 using a 6Hz electrically-induced seizure assay, which has utility to model drug-refractory epilepsy (Loscher, 2011). Using the same drug administration protocol as for the PTZ-induced seizure assay (i.e. dosing once per day/3days, then PTZ exposure), RAB216 (200mg/kg) significantly reduced the length of induced seizure in this assay ($p = 0.013$, $n = 9$, Fig. 5F). By contrast, 4-TBB (800mg/kg) did not significantly reduce seizure duration ($p = 0.1$, data not shown).

Discussion

We report here that 4-TBB and particularly its analogue RAB216, are anticonvulsants with a novel mode of action that involves up-regulation of the firing rate homeostatic regulator PUM. Firing rate neuronal homeostasis is likely to assume particular importance in epileptic circuits because of the extreme levels of activity associated with the condition. Notably though, homeostasis has never been specifically targeted for anticonvulsant control. A plausible added appeal for targeting homeostatic mechanisms is that these may be expected to impact rather less on normal physiology. This is because homeostatic mechanisms have multiple in-built protective regulatory controls that work to prevent under- or over-activation; in the case of PUM, this protein also targets its own mRNA and at least one of its cofactors (Muraro et al., 2008) As such, anticonvulsant strategies, involving neuronal homeostasis, may prove less susceptible to side effects, which are the primary reason for switching anti-epileptic medication in the clinic (Kwan et al., 2011). Observation of mice exposed to 4-TBB or RAB216, for 3 days prior to seizure induction, showed no obvious adverse effects. However, we acknowledge that future studies will be needed to screen for possible side-effects of the compounds we describe here.

Whilst multiple forms of neuronal homeostasis have been described, including synaptic scaling and presynaptic regulation of neurotransmitter release (Davis and Bezprozvanny, 2001; Turrigiano and Nelson, 2004), the compounds we describe seemingly manipulate firing rate homeostasis, which acts to maintain action potential firing within pre-determined and physiologically relevant limits (Driscoll et al., 2013). However, the effect may be more complex because it is yet to be established whether neurons utilise multiple forms of homeostasis. If this is indeed the case, then an imposed change to firing rate homeostasis may, in turn, influence synaptic scaling and/or other neuronal homeostatic mechanisms. It is also yet to be established whether all forms of neuronal homeostasis are regulated by separate or overlapping cellular mechanisms. In this regard it is notable that

ketamine and lithium are sufficient to influence synaptic scaling homeostasis (evoking up- and down-scaling, respectively), perhaps indicative that regulatory mechanisms are separable (Kavalali and Monteggia, 2020). Thus, whilst the mechanistic details remain to be resolved, our findings suggest that manipulation of homeostasis, *per se*, is a potential therapeutic target to control seizure, most likely by limiting non-physiological levels of neuronal activity.

Firing rate homeostasis is achieved, at least in part, by PUM-dependent control of voltage-gated Na⁺ channel synthesis, in both *Drosophila* and mouse (Driscoll et al., 2013; Mee et al., 2004). Analyses of Na_v protein levels, in *post-mortem* mouse brain, pre-exposed to 4-TBB, validates this mode-of action, showing reduction in Na_vs 1.1 and 1.2 but, interestingly, no change in Na_v 1.6. Intuitively, one might predict a reduction in Na_v1.6 because gain-of function mutations in the encoding gene, Na_v 1.6, are associated with hyperactivity and epilepsy (O'Brien and Meisler, 2013). By similar logic, the observed reduction of Na_v1.1 is also unexpected given that this channel type predominates in GABAergic inhibitory neurons (Catterall et al., 2010). Our analysis of these known Pum targets is, however, relatively crude in treating the whole brain as a single tissue. This approach similarly identifies reduced expression of the GLUR2 AMPA receptor subunit following exposure to 4-TBB. Again, how a reduction in this receptor subunit affects neuronal activity, particularly across the entire brain, is difficult to predict. Glutamatergic synaptic currents, in neurons with reduced expression of GLUR2, exhibit increased deactivation rates which may limit the degree of depolarization induced in the postsynaptic cell (Geiger et al., 1995). Whilst details remain to be resolved (that will require additional experiments), the changes we observe in Na_v and GLUR2 protein levels are consistent with increased PUM expression and, in this regard, serve to strengthen our hypothesis that up-regulation of this homeostatic regulator contributes to the anticonvulsant effect of 4-TBB and RAB216.

We can at present only speculate on how 4-TBB-like molecules mediate an increase in PUM expression. Indeed, in this regard, it is interesting to consider how neurons monitor their activity which, in turn, is transduced to regulate the activity status of intrinsic homeostatic mechanisms. In the case of PUM, we have reported, in *Drosophila*, that synaptic depolarization regulates expression of P300, a histone acetyltransferase that forms a complex with MEF2. As synaptic depolarization increases, levels of P300 reduce, releasing MEF2 from the complex. Once released, MEF2 binds the *dPUM* promoter and transactivates gene transcription (Lin and Baines, 2019). In mammals, by contrast, the level of MEF2 expression is itself activity-regulated, increasing with depolarization (Flavell et al., 2006), and analysis of human and mouse *PUM2* promoters identifies multiple MEF2 binding motifs (Lin and Baines, 2019). P300 is also reported to regulate MEF2 in mammals (De Luca et al., 2003), but how this protein is influenced by synaptic depolarization has not been described. In mammals, MEF2 also increases the expression of micro-RNAs, including miR-134, which is sufficient to down-regulate expression of *PUM2* (Fiore et al., 2009; Fiore et al., 2014).

Significantly, block of miR-134, using an antagomir, is anticonvulsive in rodents (Reschke et al., 2017). Thus, it is conceivable that 4-TBB, and analogues, might act at any level throughout this seemingly complex regulatory mechanism that ensures appropriate expression of PUM proteins. It is expected that levels of PUM are tightly regulated given the requirement to guard against under or over-activity of neuron activity. Indeed, these extensive regulatory and feedback controls, present in PUM-dependent homeostasis, may prove beneficial in exploiting this system for anticonvulsive therapy: minimising potential side-effects of exposure to 4-TBB or its analogues.

In summary, the study we report here provides a first proof-of-principle that manipulation of firing rate neuronal homeostasis provides a possible route to suppress seizures and, moreover, may be suitable for the treatment of patients that have drug-refractory seizures. The expression of PUM is not restricted to the CNS, being instead widespread throughout somatic tissues and, moreover, is expressed from early development (Goldstrohm et al., 2018). This raises the potential for significant side effects from drugs that act to increase expression of this protein which may limit the utility of such an approach to control seizures. Thus, targeting of CNS-specific downstream targets of PUM, or CNS-specific PUM cofactors, may prove more successful for clinical control of epilepsy. Clearly there is much work to be done before the compounds we identify could enter clinical trials, but identification of a potentially druggable neuronal homeostatic mechanism offers the exciting prospect of exploiting a novel target for the eventual control of epilepsy.

Acknowledgements

We thank Aoibhinn Kelly, Iona Hayes, Thomas Humphreys and Ceri Hughes who contributed to the 4-TBB structure-activity assay as part of their final year BSc. Projects. This work was supported by funding from the Biotechnology and Biological Sciences Research Council (BB/L027690/1 to RAB); Epilepsy Research UK (PGE2002, Explore Pilot Grant to RAB, RW and SA); an MRC-funded PhD studentship (to FM), a Wellcome Trust-NIH PhD studentship (205944/Z/17/Z to CMGS), the Vrije Universiteit Brussel (to NA and IS) and by MRC (MR/R005427/1 to AT). Work on this project benefited from the Manchester Fly Facility, established through funds from the University and the Wellcome Trust (087742/Z/08/Z).

Author contributions

Collected data: FM, WHL, CMGS, NA, YNF, GC. RP. Analyzed data: FM, WHL, CMGS, NA, RAB. Supervised experiments: IS, AT, RW, SA, SF, RAB. Wrote manuscript: RB, AT

Disclosure

None of the authors have any conflicts of interest to disclose.

Data availability statement

All research data supporting this publication are directly available within this publication.

Materials and correspondence:

Richard.Baines@manchester.ac.uk

Materials and methods

Animals: *Drosophila* were maintained at 25°C on a 16:8 light/dark cycle. Mice were housed on a 12:12 light/dark cycle at a constant ambient temperature of $21 \pm 2^\circ\text{C}$ and given access to water and standard chow ad libitum. Mouse PTZ seizure assays used male, C57BL/6J, 12-15 weeks, 23-30 g, (Charles River, UK). For the 6Hz-seizure assay, we used male NMRI mice, 10-11 weeks of age and weighing 35–45g, (Charles River, France). Drug and vehicle treatment was randomised and assays were performed by experimenters blinded to treatment. All procedures (as detailed in subsequent paragraphs below) were conducted in accordance with ARRIVE guidelines and local institutional policies and guidelines. All procedures undertaken were approved by the respective University Animal Welfare and Ethics Board (Manchester and Brussels) and conducted in accordance with respective project licence authority at each institution.

Seizure behaviour test in *Drosophila*: Wall-climbing, third-instar larvae (L3), of either sex, were subjected to an electric shock (4V DC, 3s) to induce seizure, with or without previous feeding of compound, as described (Marley and Baines, 2011). Recovery times (RT) are shown which depict the time taken for larvae to recover, evidenced by a full peristaltic wave and normal locomotion. A cut-off time of 420s was used. For compound-feeding studies, eggs were laid on food containing compound (2mM, or vehicle, 0.4% DMSO) and larvae were raised (in the presence of drug) until L3. Where experiments were conducted over a number of weeks (e.g. analogue screen shown in Fig. 4), RT was normalized to the *para*^{bss} (without compound) run each week.

dPUM:promoter assay: A *dPUM* promoter-GAL4 line (Lin and Baines, 2019) was crossed to attP24 UAS-luciferase flies (Markstein et al., 2008). Flies carrying the UAS-luciferase transgene alone were used for background controls. Adult flies were allowed to lay eggs in vials containing food with added compound (or vehicle, DMSO) and to develop to L3. Ten L3 CNSs, of either sex, were placed in 100 µl Promega Glo Lysis buffer for each sample, and 5 independent samples collected. CNSs were homogenized, incubated at room temperature (10 min), centrifuged (5 min), and supernatant transferred to a new tube. 30 µl of each sample was then transferred to a well of a white-walled 96-well plate at room temperature, 30 µl Promega Luciferase reagent was added to each well and plates incubated in the dark (10 min). Luminescence was measured with a GENios plate reader (TECAN, Reading, UK). Values were normalized to total protein concentration, measured using the Bradford protein assay (Bio-Rad, Watford, UK).

Quantitative RT-PCR: QRT-PCR was performed using a SYBR Green I real-time PCR method (Roche, LightCycler® 480 SYBR Green I Master, Mannheim, Germany) as described (Lin et al., 2015). RNA was extracted from 20 L3 CNSs per replicate, of either sex, using the RNeasy micro kit (QIAGEN, Hilden, Germany). Primer sequences (5' to 3') were: *ACTIN-5C* (CG4027), CTTCTACAATGAGCTGCGT and GAGAGCACAGCCTGGAT; *dPUM* (CG9755), GCAGCAGGGTGCCGAGAATC and CGCGGCGACCCGTCAACG (forward and reverse, respectively). These primers recognise all known splice variants of *dPUM*. Relative gene expression was calculated as the $2^{-\Delta Ct}$, where ΔCt was determined by subtracting the average *ACTIN-5C* Ct value from that of *dPUM*. The ratio of target gene expression to house-keeping *ACTIN-5C* gene (i.e. raw data) was compared across control vs. experimental tissue.

Organotypic slice cultures: Slice cultures were prepared from 5 to 9 day old C57BL/6J mouse pups, of either sex, according to the interface organotypic culture method (Gogolla et al., 2006; Stoppini et al., 1991). Brains were removed and hippocampi dissected and transversely sectioned into 350 µm slices (McIlwain tissue chopper). Slices were plated on polyester membrane inserts (0.4 µm pore) in 6 well culture plates (Corning Costar CLS3450-24EA, Sigma-Aldrich, UK), 2-3 slices per insert, containing 1.2ml of feeding media (50% Minimum Essential Media + GlutaMAX, phenol red and with Earle's salts (Fisher Scientific, Loughborough, UK), 25 % heat-inactivated horse serum (Sigma, Poole, UK), 21.56 % EBSS, 2 % B27 serum (Fisher Scientific) and 36 mM D-Glucose. Slices were kept at 37°C / 5% CO₂ and the media replaced the day after plating and then 2-3 times weekly depending on plating density. This method of preparing organotypic hippocampal slice cultures induces spontaneous epileptic-like activity without the need for any pharmacological or electrical provocation (Berdichevsky et al., 2012; Ellender et al., 2014; Lillis et al., 2012; Liu et

al., 2017). The slicing process mimics a traumatic brain injury which leads to cell death, deafferentation and subsequent axonal sprouting – all of which contribute towards the gradual development of seizure-like activity (McBain et al., 1989).

Local field potentials, at Days In Vitro (DIV) 7-14, were recorded in CA1, in organotypic cultures, using glass borosilicate patch pipettes (~1-3M Ω , Harvard Apparatus, Kent, UK) and a Multiclamp 700B (Molecular Devices, CA, USA). Slices were perfused with oxygenated ACSF (125 mM NaCl, 26 mM NaHCO₃, 10 mM glucose, 3.5 mM KCl, 1.26 mM NaH₂PO₄, 2 mM CaCl₂, 1 mM MgCl₂) and maintained at 33–36°C for 7 hours. The first hour was used as an activity baseline: slices lacking seizure-like discharges during this period were discarded. After the first hour of baseline activity, slices were bathed in media supplemented with 4-TBB (1.2 mM). Analysis was performed using MATLAB (The MathWorks Inc., Natick, MA, USA). Signals were digitised using a 1401-3 AD converter (Cambridge Electronic Design), and recorded using Spike2 software (Cambridge Electronic Design, version 7) with sampling rate of 10 kHz. 50 Hz noise was removed using an in-built Spike2 software tool and recordings were discarded if the signal:noise ratio was too great to clearly distinguish events from baseline activity. Interictal events were designated as brief (<1 second), large amplitude deflections in the LFP trace with a spike and wave discharge pattern. Ictal activity ("seizure-like events", SLEs) followed a similar initial large amplitude spike and wave discharge followed by a period of after-discharge activity persisting for several to tens of seconds. SLEs were defined as continual discharges lasting > 5 seconds.

PTZ seizure-induction: Mice injected subcutaneously (sc.) with 0.1 ml of compound (in NaCl, 0.9% w/v saline) or saline vehicle, once per day for 3 days. Four hours after the last injection on day 3, a single dose of PTZ (60 mg/kg/sc. in saline.) was injected. Each mouse was placed into a separate clear plastic arena and videoed for 20 min. After the observation period, mice were anesthetized with isoflurane (3-4% in 20% O₂ and 50% N₂O, 0.5 l/min), transcardially perfused with 0.9% saline and brains removed and stored at -80°C. Seizure scoring was carried out from videos, independently scored by two experimenters blinded to the experimental groups until full analysis was complete. Concordance between the two experimenters was high (\leq 5% difference for timings) and averaged values were taken forward for statistical analysis. Scoring was based on identification of 2 clear behaviours from a modified Racine score of 3 (Straub tail) and 5 (rearing and falling) (Racine, 1972).

6Hz seizure-induction: Prior to the electrical stimulation, 0.5% xylocaine was applied to the cornea to induce local anesthesia and ensure good conductivity. Corneal stimulation (46 mA, 0.2 ms

duration pulses at 6 Hz for 3 s) was administered by a constant current device (ECT Unit 57800; Ugo Basile, Comerio, Italy) (Aourz et al., 2019; Walrave et al., 2018). Acutely evoked 6-Hz seizures were characterized by stun, forelimb clonus, twitching of vibrissae, and/or Straub-tail. For each animal, the total seizure duration was manually recorded. Ip administration of levetiracetam (LEV, 100mg/kg) 1h before seizure induction was used as a positive control (Walrave et al., 2015). Seizure scoring was carried out live during the experiment. The entire experiment was also video recorded for confirmation of timings if required. For these experiments, the sole researcher was blinded to the experimental groups until full analysis was complete.

Western blot: Whole brain was homogenised in ice-cold buffer (150 mM NaCl, 50 mM Tris-HCl, 1% Nonidet P-40, 0.5% Sodium deoxycholate and 0.1% SDS) containing protease inhibitors (Promega, Madison, USA) and centrifuged at 10,000× g (30 min at 4°C). Supernatant was stored at -20°C. Antibodies were: anti-PUM 1 (1:1000, #12322, Cell Signaling, MA, USA), anti-PUM 2 (1:1000, ab10361, Abcam, Cambridge, UK), anti-SCN1A (1:1000, ASC-001, alomone labs, Jerusalem, Israel), anti-SCN2A (1:1000, ASC-002, alomone labs), anti-SCN8A (1: 1000, ASC-009, alomone labs), anti-GluR2 (1:2000, AB1768-I, Merck, Darmstadt, Germany) and anti-β-Actin (1:5000, ab8227, Abcam). Samples (25 µg of protein) were separated by SDS page, and protein transferred to a polyvinylidene difluoride membrane (GE Healthcare). After blocking (0.5 % BSA and 0.05% TWEEN-20 in Tris-buffered saline, TBS-T), membrane was incubated overnight (4°C) in primary antibody diluted in 0.5% BSA in TBS-T. Membranes were incubated with HRP-conjugated secondary antibodies (1:2500, #7074, Cell Signaling) in 0.3% BSA in TBS-T and blots developed with an Enhanced Chemiluminescent Detection Kit (Pierce, Rockford, USA). Protein band density was measured using Image J (NIH, USA).

Chemical analogues: RAB216 was designed by first screening analogues of 4-TBB and its carboxylic acid derivative RAB102. The structure activity relationship (SAR) revealed that only compounds with a carboxylic acid or aldehyde group directly bonded to the benzene ring were active, even when replaced with isosteric groups. Furthermore, a change of the benzene ring to a pyridine or indole ring, or a change of substituents from para to meta, resulted in complete loss of activity. Electronegative groups were tolerated in the para-position, increasing the likelihood of a compound forming strong intermolecular bonds with its binding partner. Therefore, when designing the second-generation compounds (sTable 1), some analogues included electronegative oxygen and nitrogen atoms. This included RAB216 which contained a pyrazole ring, providing extra interactions to enhance activity. Additionally, analysis of the screen showed that compounds with an element of 3D structure were more active: in RAB216 the two methyl groups attached to the

pyrazole group caused it to be twisted by approximately 18°. Reviews of drug libraries suggest that planar compounds are less likely to be biologically active (Lovering et al., 2009). Compounds, including RAB216, were designed in accordance with Lipinski's rules, such as molecular weight (under 500) and lipophilicity (logP under 5), to give desirable physiochemical properties (Lipinski et al., 2001). All of the compounds screened, including RAB216, fit within these guidelines (sTable 1).

Chemical synthesis

4-(3,5-Dimethyl-1H-pyrazol-4-yl)benzoic acid (RAB216): 4-Iodobenzoic acid (4.46 g, 20 mmol), copper(I) iodide (0.381 g, 2 mmol), L-proline (0.460 g, 4 mmol) and K₂CO₃ (11.10 g, 80 mmol) were suspended in dry dimethyl sulfoxide (100 mL) under an argon atmosphere and stirred for 10 minutes at room temperature. 2,4-Pentanedione (6.2 mL, 60 mmol) was added dropwise to this mixture, which was heated to 90 °C and stirred for 24 hours. After cooling to room temperature, the mixture was transferred slowly and with stirring into hydrochloric acid (3 M, 250 mL). An additional 150 mL of water was added, and the mixture was cooled in an ice bath causing a precipitate to form. After filtration and washing with ice-cooled water (3x 100 mL) the filter cake was dried in an oven to give 3-(4-carboxyphenyl)-2,4-pentanedione (3.60 g) as a crude product. The compound was taken forward to the next step without purification due to co-elution seen by TLC.

A solution of crude 3-(4-carboxyphenyl)-2,4-pentanedione (3.24 g, 15 mmol) in ethanol (40 mL) was added dropwise to a solution of hydrazine monohydrate (1.75 g, 20 mmol) in ethanol (10 mL) while stirring. Upon complete addition the combined solution was then heated at reflux for 1 h. After cooling to room temperature, the solvent was removed under reduced pressure to give the crude product. The product was purified by silica gel chromatography (85% EtOAc in hexane) to give 4-(3,5-Dimethyl-1H-pyrazol-4-yl)benzoic acid ¹H NMR (500 MHz, DMSO-d₆) δ 12.63 (s, 1H, COOH), 12.63 (s, 1H, NH), 7.96 (d, 2H), 7.42 (d, J = 8.5, 2H), 2.24 (s, 6H). ¹³C NMR (126 MHz, DMSO-d₆): δ 11.6; 127-130; 138.8; 167.5. MS (ES⁺, m/z) 217.1.

4-(1H-Pyrrol-2-yl)benzoic acid (RAB211); A solution of Na₂CO₃ (1.83 g, 17.3 mmol) in water (10 mL) was added to 1-tert-butoxycarbonylpyrrole-2-boronic acid (1.04 g, 4.88 mmol), 4-carboxyiodobenzene (1g, 4.04 mmol), and tetrakis(triphenylphosphine)palladium(0) (0.30 g, 0.257 mmol) in THF (60 mL) under argon. The mixture was heated at 45 °C for 2 h and cooled to room temperature. 2 M HCl was added until the solution reached pH 3. The product was extracted with ethyl acetate (3 x 50 mL) and washed with 0.1 M HCl (3 x 20 mL). The solution was dried over MgSO₄ and the solvent was removed in vacuo to give 4-(1-(tert-butoxycarbonyl)-1H-pyrrol-2-yl)benzoic acid, which was dissolved in DMSO (20 mL) and heated to 150 °C for 30 min. The

solution was cooled to room temperature and 0.1 M HCl (50 mL) was added. The product was extracted with ethyl acetate (3 x 100 mL) and washed with 0.1 M HCl (3 x 30 mL). The solution was dried over MgSO₄ and the solvent was removed in vacuo. The product was purified by silica gel chromatography (6% MeOH/CH₂Cl₂) to give 4-(1H-pyrrol-2-yl)benzoic acid (0.53 g, yield 70%) ¹H NMR (400 MHz, DMSO-d₆) δ 12.76 (s, 1H), 11.50 (s, 1H), 7.90 (d, J = 8.7 Hz, 2H), 7.72 (d, J = 8.7 Hz, 2H), 6.94 (td, J = 2.7, 1.4 Hz, 1H), 6.69 (ddd, J = 3.9, 2.5, 1.5 Hz, 1H), 6.17 (dt, J = 3.5, 2.3 Hz, 1H). MS (ES⁺, m/z) 188.05.

4-(Dimethylcarbamoyl)benzoic acid (RAB212): Methyl 4-chlorocarbonylbenzoate (1 g, 5 mmol), was dissolved in DCM (20 mL) and a solution of dimethyl ammonium chloride (0.61 g, 7.5 mmol) and triethylamine (1.05 mL, 7.5 mmol) was added slowly with stirring. The reaction was left for 1 h and the product was extracted with DCM (3 x 25 mL) and then washed with water (3 x 20 mL). The solvent was removed in vacuo to give methyl 4-(dimethylcarbamoyl)benzoate as a crude product. The crude product was taken forward to the next step without further purification. Crude methyl 4-(dimethylcarbamoyl) benzoate was dissolved in THF (50 mL) and a solution of LiOH (1 g) in water (50 mL) was added and the solution was stirred at room temperature for 16 h. HCl was added to the solution with stirring until the solution reached pH 3. The product was extracted with ethyl acetate (3 x 50 mL) and washed with 0.1 M HCl (3 x 30 mL) before the solvent was removed in vacuo to give 4-(dimethylcarbamoyl) benzoic acid (0.80 g, yield 83% over two steps) ¹H NMR (400 MHz, DMSO-d₆) δ 7.86 (d, J = 7.7 Hz, 2H), 7.27 (d, J = 7.7 Hz, 2H), 2.97 (s, 3H), 2.90 (s, 3H). MS (ES⁺, m/z) 194.08.

Statistics: No data points were excluded from analysis. Following demonstration of normality of raw data, statistical significance was tested using either a Student's two-tailed *t*-test (paired or unpaired), a one-way or two-way ANOVA followed by correction for multiple comparisons, or a Fishers exact test (actual test used identified in respective figure legend). For QRT-PCR data, statistical analysis was performed on raw data (i.e ratio of target gene to *ACTIN-5C*), prior to normalising for graphical display. Level of significance on figures is indicated by * ($p \leq 0.05$), ** ($p \leq 0.01$), *** ($p \leq 0.001$). Figures show means \pm SD.

References

- Aourz, N., Serruys, A. K., Chabwine, J. N., Balegamire, P. B., Afrikanova, T., Edrada-Ebel, R., Grey, A. I., Kamuhabwa, A. R., Walrave, L., Esguerra, C. V. et al.** (2019). Identification of GSK-3 as a Potential Therapeutic Entry Point for Epilepsy. *ACS chemical neuroscience* **10**, 1992-2003.
- Arvola, R. M., Weidmann, C. A., Tanaka Hall, T. M. and Goldstrohm, A. C.** (2017). Combinatorial control of messenger RNAs by Pumilio, Nanos and Brain Tumor Proteins. *RNA Biol*, 1-12.
- Baines, R. A., Giachello, C. N. G. and Lin, W. H.** (2017). *Drosophila. Models of Seizures and Epilepsy, 2nd Edition*, 345-358.
- Berdichevsky, Y., Dzhala, V., Mail, M. and Staley, K. J.** (2012). Interictal spikes, seizures and ictal cell death are not necessary for post-traumatic epileptogenesis in vitro. *Neurobiol Dis* **45**, 774-85.
- Bohn, J. A., Van Etten, J. L., Schagat, T. L., Bowman, B. M., McEachin, R. C., Freddolino, P. L. and Goldstrohm, A. C.** (2018). Identification of diverse target RNAs that are functionally regulated by human Pumilio proteins. *Nucleic Acids Res* **46**, 362-386.
- Catterall, W. A., Kalume, F. and Oakley, J. C.** (2010). Nav1.1 channels and epilepsy. *The Journal of physiology* **588**, 1849-59.
- Chen, C. R., Tan, R., Qu, W. M., Wu, Z., Wang, Y., Urade, Y. and Huang, Z. L.** (2011). Magnolol, a major bioactive constituent of the bark of *Magnolia officinalis*, exerts antiepileptic effects via the GABA/benzodiazepine receptor complex in mice. *Br J Pharmacol* **164**, 1534-46.
- Davis, G. W. and Bezprozvanny, I.** (2001). Maintaining the stability of neural function: a homeostatic hypothesis. *Annual review of physiology* **63**, 847-69.
- De Luca, A., Severino, A., De Paolis, P., Cottone, G., De Luca, L., De Falco, M., Porcellini, A., Volpe, M. and Condorelli, G.** (2003). p300/cAMP-response-element-binding-protein ('CREB')-binding protein (CBP) modulates co-operation between myocyte enhancer factor 2A (MEF2A) and thyroid hormone receptor-retinoid X receptor. *The Biochemical journal* **369**, 477-84.
- Dong, H., Zhu, M., Meng, L., Ding, Y., Yang, D., Zhang, S., Qiang, W., Fisher, D. W. and Xu, E. Y.** (2018). Pumilio2 regulates synaptic plasticity via translational repression of synaptic receptors in mice. *Oncotarget* **9**, 32134-32148.
- Driscoll, H. E., Muraro, N. I., He, M. and Baines, R. A.** (2013). Pumilio-2 regulates translation of nav1.6 to mediate homeostasis of membrane excitability. *The Journal of Neuroscience* **33**, 9644-54.
- Ellender, T. J., Raimondo, J. V., Irkle, A., Lamsa, K. P. and Akerman, C. J.** (2014). Excitatory effects of parvalbumin-expressing interneurons maintain hippocampal epileptiform activity via synchronous afterdischarges. *J Neurosci* **34**, 15208-22.
- Erdtmann-Vourliotis, M., Riechert, U., Mayer, P., Grecksch, G. and Holtt, V.** (1998). Pentylentetrazole (PTZ)-induced c-fos expression in the hippocampus of kindled rats is suppressed by concomitant treatment with naloxone. *Brain Res* **792**, 299-308.
- Fiore, R., Khudayberdiev, S., Christensen, M., Siegel, G., Flavell, S. W., Kim, T. K., Greenberg, M. E. and Schratt, G.** (2009). Mef2-mediated transcription of the miR379-410 cluster regulates activity-dependent dendritogenesis by fine-tuning Pumilio2 protein levels. *The EMBO journal* **28**, 697-710.
- Fiore, R., Rajman, M., Schwale, C., Bicker, S., Antoniou, A., Bruehl, C., Draguhn, A. and Schratt, G.** (2014). MiR-134-dependent regulation of Pumilio-2 is necessary for homeostatic synaptic depression. *The EMBO journal* **33**, 2231-46.
- Flavell, S. W., Cowan, C. W., Kim, T. K., Greer, P. L., Lin, Y., Paradis, S., Griffith, E. C., Hu, L. S., Chen, C. and Greenberg, M. E.** (2006). Activity-dependent regulation of MEF2 transcription factors suppresses excitatory synapse number. *Science* **311**, 1008-12.
- Follwaczny, P., Schieweck, R., Riedemann, T., Demleitner, A., Straub, T., Klemm, A. H., Bilban, M., Sutor, B., Popper, B. and Kiebler, M. A.** (2017). Pumilio2-deficient mice show a predisposition for epilepsy. *Dis Model Mech* **10**, 1333-1342.
- Galgano, A., Forrer, M., Jaskiewicz, L., Kanitz, A., Zavolan, M. and Gerber, A. P.** (2008). Comparative analysis of mRNA targets for human PUF-family proteins suggests extensive interaction with the miRNA regulatory system. *PLoS ONE* **3**, e3164.
- Geiger, J. R., Melcher, T., Koh, D. S., Sakmann, B., Seeburg, P. H., Jonas, P. and Monyer, H.** (1995). Relative abundance of subunit mRNAs determines gating and Ca²⁺ permeability of AMPA receptors in principal neurons and interneurons in rat CNS. *Neuron* **15**, 193-204.

Gennarino, V. A., Singh, R. K., White, J. J., De Maio, A., Han, K., Kim, J. Y., Jafar-Nejad, P., di Ronza, A., Kang, H., Sayegh, L. S. et al. (2015). Pumilio1 haploinsufficiency leads to SCA1-like neurodegeneration by increasing wild-type Ataxin1 levels. *Cell* **160**, 1087-98.

Gerber, A. P., Luschnig, S., Krasnow, M. A., Brown, P. O. and Herschlag, D. (2006). Genome-wide identification of mRNAs associated with the translational regulator PUMILIO in *Drosophila melanogaster*. *Proceedings of the National Academy of Sciences of the United States of America* **103**, 4487-92.

Giachello, C. N. and Baines, R. A. (2017). Regulation of motoneuron excitability and the setting of homeostatic limits. *Current opinion in neurobiology* **43**, 1-6.

Gogolla, N., Galimberti, I., DePaola, V. and Caroni, P. (2006). Preparation of organotypic hippocampal slice cultures for long-term live imaging. *Nat Protoc* **1**, 1165-71.

Goldstrohm, A. C., Hall, T. M. T. and McKenney, K. M. (2018). Post-transcriptional Regulatory Functions of Mammalian Pumilio Proteins. *Trends Genet* **34**, 972-990.

Hogan, G. J., Brown, P. O. and Herschlag, D. (2015). Evolutionary Conservation and Diversification of Puf RNA Binding Proteins and Their mRNA Targets. *PLoS biology* **13**, e1002307.

Kavalali, E. T. and Monteggia, L. M. (2020). Targeting Homeostatic Synaptic Plasticity for Treatment of Mood Disorders. *Neuron* **106**, 715-726.

Kwan, P., Schachter, S. C. and Brodie, M. J. (2011). Drug-resistant epilepsy. *N Engl J Med* **365**, 919-26.

Lillis, K. P., Kramer, M. A., Mertz, J., Staley, K. J. and White, J. A. (2012). Pyramidal cells accumulate chloride at seizure onset. *Neurobiol Dis* **47**, 358-66.

Lin, W. H. and Baines, R. A. (2019). Myocyte enhancer factor-2 and p300 interact to regulate the expression of homeostatic regulator Pumilio in *Drosophila*. *The European journal of neuroscience*.

Lin, W. H., Giachello, C. N. and Baines, R. A. (2017). Seizure control through genetic and pharmacological manipulation of Pumilio in *Drosophila*: a key component of neuronal homeostasis. *Dis Model Mech* **10**, 141-150.

Lin, W. H., He, M. and Baines, R. A. (2015). Seizure suppression through manipulating splicing of a voltage-gated sodium channel. *Brain : a journal of neurology* **138**, 891-901.

Lipinski, C. A., Lombardo, F., Dominy, B. W. and Feeney, P. J. (2001). Experimental and computational approaches to estimate solubility and permeability in drug discovery and development settings. *Adv Drug Deliv Rev* **46**, 3-26.

Liu, J., Saponjian, Y., Mahoney, M. M., Staley, K. J. and Berdichevsky, Y. (2017). Epileptogenesis in organotypic hippocampal cultures has limited dependence on culture medium composition. *PLoS ONE* **12**, e0172677.

Loscher, W. (2011). Critical review of current animal models of seizures and epilepsy used in the discovery and development of new antiepileptic drugs. *Seizure* **20**, 359-68.

Lovering, F., Bikker, J. and Humblet, C. (2009). Escape from flatland: increasing saturation as an approach to improving clinical success. *J Med Chem* **52**, 6752-6.

Markstein, M., Pitsouli, C., Villalta, C., Celniker, S. E. and Perrimon, N. (2008). Exploiting position effects and the gypsy retrovirus insulator to engineer precisely expressed transgenes. *Nat Genet* **40**, 476-83.

Marley, R. and Baines, R. A. (2011). Increased persistent Na⁺ current contributes to seizure in the slamdance bang-sensitive *Drosophila* mutant. *Journal of neurophysiology* **106**, 18-29.

McBain, C. J., Boden, P. and Hill, R. G. (1989). Rat hippocampal slices 'in vitro' display spontaneous epileptiform activity following long-term organotypic culture. *J Neurosci Methods* **27**, 35-49.

Mee, C. J., Pym, E. C., Moffat, K. G. and Baines, R. A. (2004). Regulation of neuronal excitability through pumilio-dependent control of a sodium channel gene. *J Neurosci* **24**, 8695-703.

Muraro, N. I., Weston, A. J., Gerber, A. P., Luschnig, S., Moffat, K. G. and Baines, R. A. (2008). Pumilio binds para mRNA and requires Nanos and Brat to regulate sodium current in *Drosophila* motoneurons. *J Neurosci* **28**, 2099-109.

O'Brien, J. E. and Meisler, M. H. (2013). Sodium channel SCN8A (Nav1.6): properties and de novo mutations in epileptic encephalopathy and intellectual disability. *Front Genet* **4**, 213.

Patsalos, P. N. (2015). The clinical pharmacology profile of the new antiepileptic drug perampanel: A novel noncompetitive AMPA receptor antagonist. *Epilepsia* **56**, 12-27.

Racine, R. J. (1972). Modification of seizure activity by electrical stimulation. II. Motor seizure. *Electroencephalogr Clin Neurophysiol* **32**, 281-94.

Reschke, C. R., Silva, L. F., Norwood, B. A., Senthilkumar, K., Morris, G., Sanz-Rodriguez, A., Conroy, R. M., Costard, L., Neubert, V., Bauer, S. et al. (2017). Potent Anti-seizure Effects of Locked Nucleic Acid Antagomirs Targeting miR-134 in Multiple Mouse and Rat Models of Epilepsy. *Mol Ther Nucleic Acids* **6**, 45-56.

Siemen, H., Colas, D., Heller, H. C., Brustle, O. and Pera, R. A. (2011). Pumilio-2 function in the mouse nervous system. *PLoS ONE* **6**, e25932.

Stoppini, L., Buchs, P. A. and Muller, D. (1991). A simple method for organotypic cultures of nervous tissue. *J Neurosci Methods* **37**, 173-82.

Turrigiano, G. G. and Nelson, S. B. (2004). Homeostatic plasticity in the developing nervous system. *Nature reviews. Neuroscience* **5**, 97-107.

Vessey, J. P., Schoderboeck, L., Gingl, E., Luzi, E., Riefler, J., Di Leva, F., Karra, D., Thomas, S., Kiebler, M. A. and Macchi, P. (2010). Mammalian Pumilio 2 regulates dendrite morphogenesis and synaptic function. *Proceedings of the National Academy of Sciences of the United States of America* **107**, 3222-7.

Walrave, L., Maes, K., Coppens, J., Bentea, E., Van Eeckhaut, A., Massie, A., Van Liefferinge, J. and Smolders, I. (2015). Validation of the 6 Hz refractory seizure mouse model for intracerebroventricularly administered compounds. *Epilepsy research* **115**, 67-72.

Walrave, L., Pierre, A., Albertini, G., Aourz, N., De Bundel, D., Van Eeckhaut, A., Vinken, M., Giaume, C., Leybaert, L. and Smolders, I. (2018). Inhibition of astroglial connexin43 hemichannels with TAT-Gap19 exerts anticonvulsant effects in rodents. *Glia* **66**, 1788-1804.

Wu, X. L., Huang, H., Huang, Y. Y., Yuan, J. X., Zhou, X. and Chen, Y. M. (2015). Reduced Pumilio-2 expression in patients with temporal lobe epilepsy and in the lithium-pilocarpine induced epilepsy rat model. *Epilepsy & behavior : E&B* **50**, 31-39.

Yaari, Y., Selzer, M. E. and Pincus, J. H. (1986). Phenytoin: mechanisms of its anticonvulsant action. *Ann Neurol* **20**, 171-84.

Zhang, M., Chen, D., Xia, J., Han, W., Cui, X., Neuenkirchen, N., Hermes, G., Sestan, N. and Lin, H. (2017). Post-transcriptional regulation of mouse neurogenesis by Pumilio proteins. *Genes & development* **31**, 1354-1369.

Figures and Tables

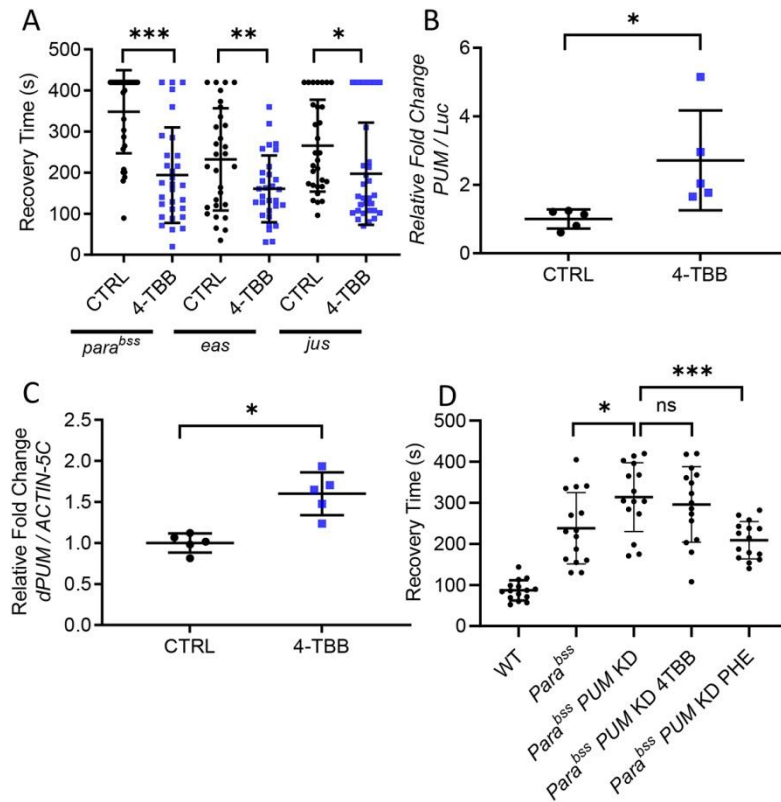


Fig. 1. 4-TBB is anticonvulsant in *Drosophila*.

A) An anticonvulsant effect of 4-TBB is present in three independent *Drosophila* seizure mutations, *para^{bss}* ($p < 0.001$), *eas* ($p = 0.011$) and *jus* ($p = 0.03$) (unpaired t -tests, $n = 30$ larvae for each treatment). **B)** Identical exposure of transgenic *dpum*-promoter-GAL4>UAS-Luciferase (Luc) larvae to 4-TBB results in significant up-regulation of Luc expression ($p = 0.03$, unpaired t -test, $n = 5$ independent samples / 10 CNS per sample). **C)** Ingestion of 4-TBB is sufficient to increase *dpUM* mRNA abundance measured by QRT-PCR ($p = 0.002$, unpaired t -test, $n = 5$ independent samples / 20 CNS per sample). **D)** RNAi-mediated knockdown of *dpUM* expression in *para^{bss}* expectedly increases seizure recovery time (Lin et al., 2017) ($p = 0.03$). Exposure to 4-TBB is ineffective in this background ($p = 0.87$), whilst exposure to phenytoin (PHE, 2mM in food) remains anticonvulsant ($p = 0.002$). Significance tested using a one-way ANOVA ($F_{(4, 70)} = 24$, $p = 0.0009$) with correction for multiple comparisons (Dunnett's). Wildtype (WT) recovery time is shown for comparison. Bars report means \pm SD ($n = 15$). * = $p < 0.05$, ** = $p < 0.01$, *** = $p < 0.001$, ns = not significant.

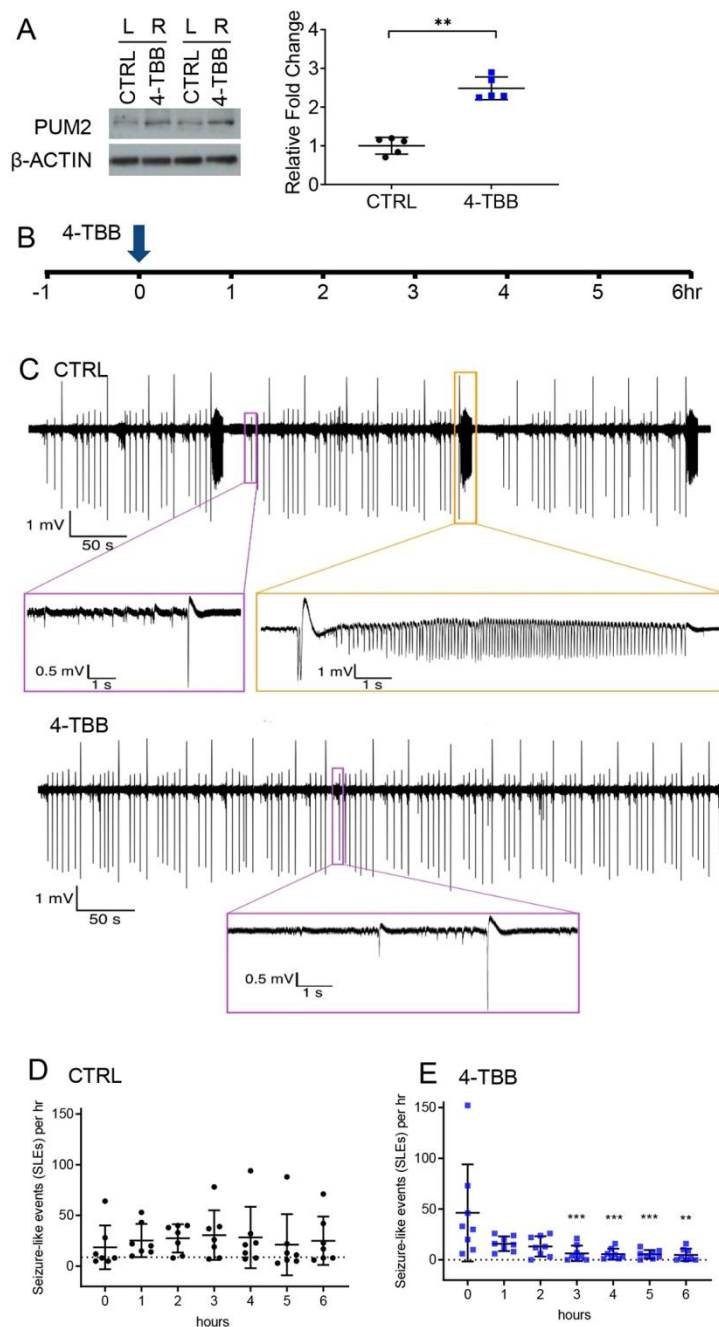


Fig. 2. 4-TBB is anticonvulsant in mouse organotypic hippocampal slice cultures.

A) Incubation (2hr) of mouse brain slice with 4-TBB (1.2mM) is sufficient to increase expression of PUM2 protein. An example Western Blot is shown where the equivalent brain slice, from either hemisphere, was exposed to vehicle (slice from left hemisphere) or drug (slice from right hemisphere). The analysis was repeated 5 independent times and this data is shown in the graph ($P = 0.003$, paired t-test). **B)** Hippocampal slices (7-14 DIV) that exhibited epileptiform activity were exposed to 4-TBB (1.2mM in bathing saline) at time '0' during a 7 hr recording period. **C)** Representative extracellular recordings of local field potentials (LFPs) showing seizure-like activity in CA1 region of DIV 10 hippocampal slice culture at baseline (CTRL) and 3 hours after 4-TBB application (4-TBB). Slice cultures at baseline, and untreated slice cultures throughout the recording period, exhibited short duration interictal spikes (purple boxes), and longer duration ictal-like events (orange boxes). In this example, 4-TBB treatment eliminated the presence of the longer duration ictal-like events. **D)** An analysis of the number of seizure-like events (SLEs, ictal-like events lasting > 5 seconds) in untreated slices (CTRL) shows robust epileptiform activity throughout the

recording period. **E)** 4-TBB significantly reduces the frequency of these SLEs, $n = 7$ (CTRL) and $n = 8$ (4-TBB) independent slices, respectively. Significance for the effect of 4-TBB *vs.* CTRL was tested using a two-way ANOVA ($F_{(13, 84)} = 5.823, p < 0.0001$). Analysis of the effect of 4-TBB shows that the reduction in epileptiform activity is significant from 3 hrs onwards ($F_{(13, 91)} = 2.473, p = 0.0063$ with correction for multiple comparisons (Šídák's)). Bars show means \pm SD. ** = $p < 0.01$, *** = $p < 0.001$.

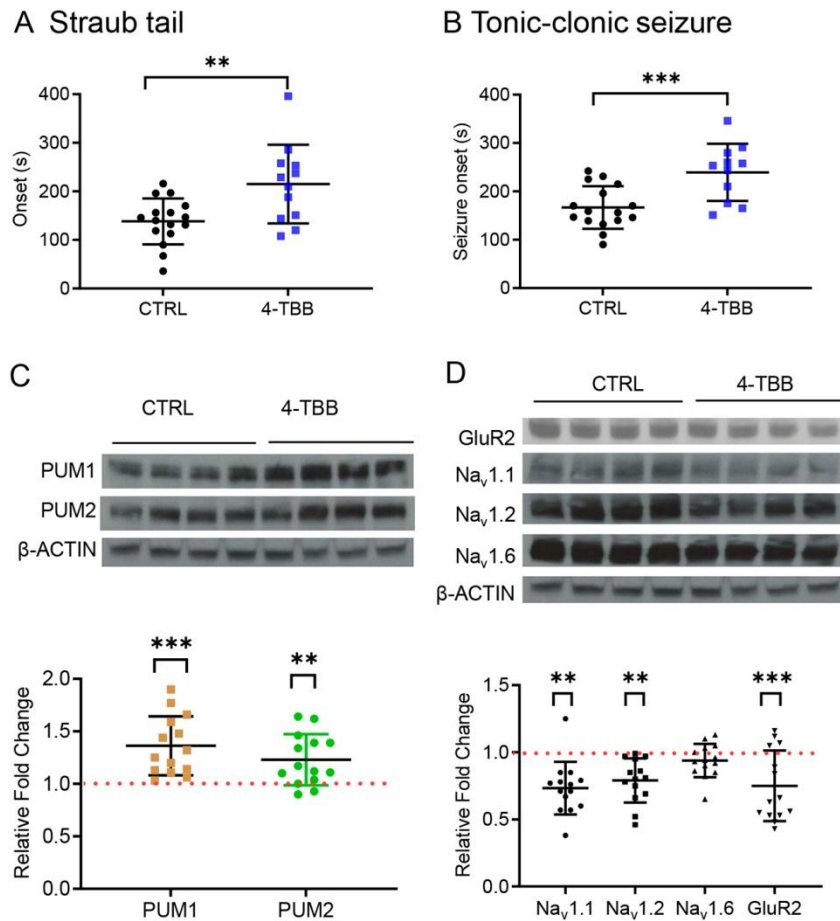


Fig. 3. 4-TBB is anticonvulsant in the mouse PTZ-induced seizure model.

Exposure to 4-TBB increases time to onset of **A**) Straub tail ($p = 0.004$) and **B**) generalised tonic-clonic seizure ($p = 0.001$). **C**). *Post-mortem* analysis of brains, taken from the mice used in the assay, shows expression of PUM1 ($p < 0.0001$) and PUM2 ($p = 0.01$), is up-regulated in animals treated with 4-TBB compared to controls (set as 1). Bars show means \pm SD. Inset shows an example Western Blot. Significance was tested in A - C using unpaired *t*-tests. **D**) Western Blot analysis of Na_v1.1, 1.2, 1.6 and GLUR2 expression in mouse brain show that exposure to 4-TBB is sufficient to down-regulate Na_v1.1 ($p = 0.005$), 1.2 ($p = 0.007$), and GLUR2 ($p = 0.001$), but not Na_v1.6 ($p = 0.75$). $n = 14$, Bars show means \pm SD. Significance was tested using ANOVA ($F_{(4, 65)} = 6.7$, $p = 0.0001$) with correction for multiple comparisons (Dunnett's). Inset shows an example Western Blot. ** = $p < 0.01$, *** = $p < 0.001$

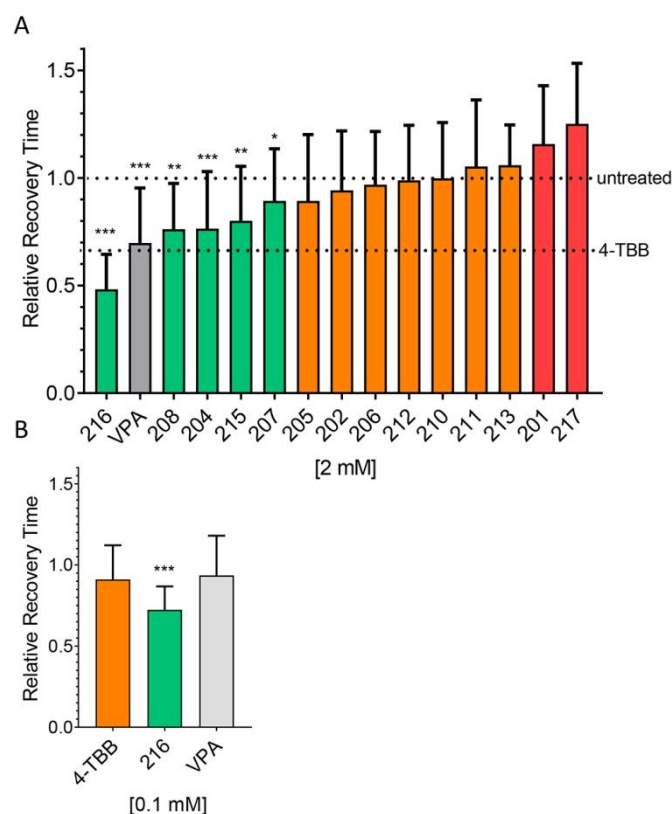


Fig. 4. Identification of a more active 4-TBB analogue.

A) 4-TBB analogues (structures shown in sTable 1) identified a number of active compounds, of which 4-(3,5-dimethyl-1*H*-pyrazol-4-yl) benzoic acid (RAB216) was the most potent. Relative recovery time (recovery time normalised to *para*^{bss} run at the same time as drugs) was calculated as a ratio of the treatment group (*para*^{bss} + compound) recovery time compared to the corresponding untreated group (*para*^{bss} - compound) from that week of screening. Green denotes a significant reduction in recovery time, orange denotes no change and red a proconvulsant effect. Sodium valproate (VPA, gray bar) was included as an additional control. * = $p < 0.05$, ** = $p < 0.01$, *** = $p < 0.001$ (individual unpaired *t*-tests, between *para*^{bss} - compound vs. *para*^{bss} + compound). **B)** RAB216 remained active at the reduced concentration of 0.1 mM, whilst both 4-TBB and VPA (tested at the same time) were inactive at this reduced level. Effect of RAB216 significant at $p < 0.001$ compared to 4-TBB (one-way ANOVA ($F_{(2, 89)} = 3.9$) followed by correction for multiple comparisons (Dunnett's).

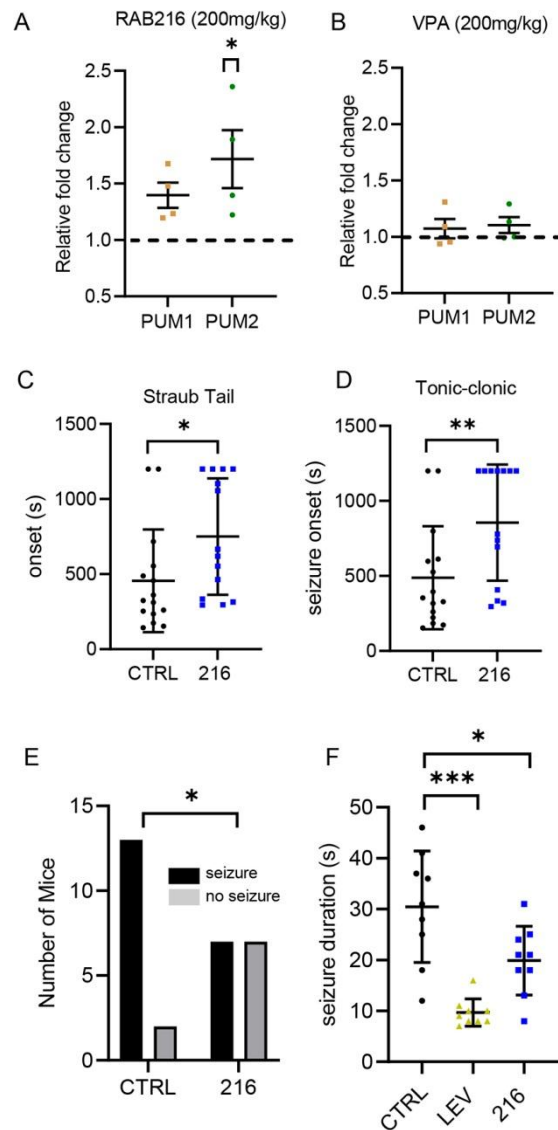


Fig. 5. Characterisation of RAB216 shows it to be more potent than 4-TBB

A) Western blot analysis of the effect of exposure of mouse brain to RAB216 on PUM1 ($n = 4$, $p = 0.07$) and PUM2 ($n = 4$, $p = 0.01$) expression (unpaired t -tests). **B)** Sodium valproate (VPA), which is an effective anticonvulsant in this assay, had no effect on expression of PUM1 or 2 ($n = 4$, $p > 0.05$). **C)** Effect of RAB216 on Straub tail ($p = 0.03$) and **D)** first appearance of a tonic-clonic seizure ($p = 0.01$) in the PTZ-induced seizure assay. Timings were capped at 20 min (1200 sec). $N = 15$, (unpaired t -tests). **E)** Percentage animals exposed to PTZ showing tonic-clonic seizure following exposure to either saline (CTRL) or RAB216 ($p = 0.05$) respectively, ($n = 15$ and 14 , respectively, Fishers exact test). **F)** Exposure to RAB216 reduces 6Hz electrically-induced seizure duration ($n = 9$ $p = 0.013$). Levetiracetam (LEV, 100mg/kg, $n = 9$, $p < 0.0001$) was used as a positive control with known efficacy in this assay. Significance was tested using ANOVA ($F_{(2, 24)} = 16.88$) with correction for multiple comparisons (Dunnett's). * = $p < 0.05$, ** = $p < 0.01$, *** = $p < 0.001$.

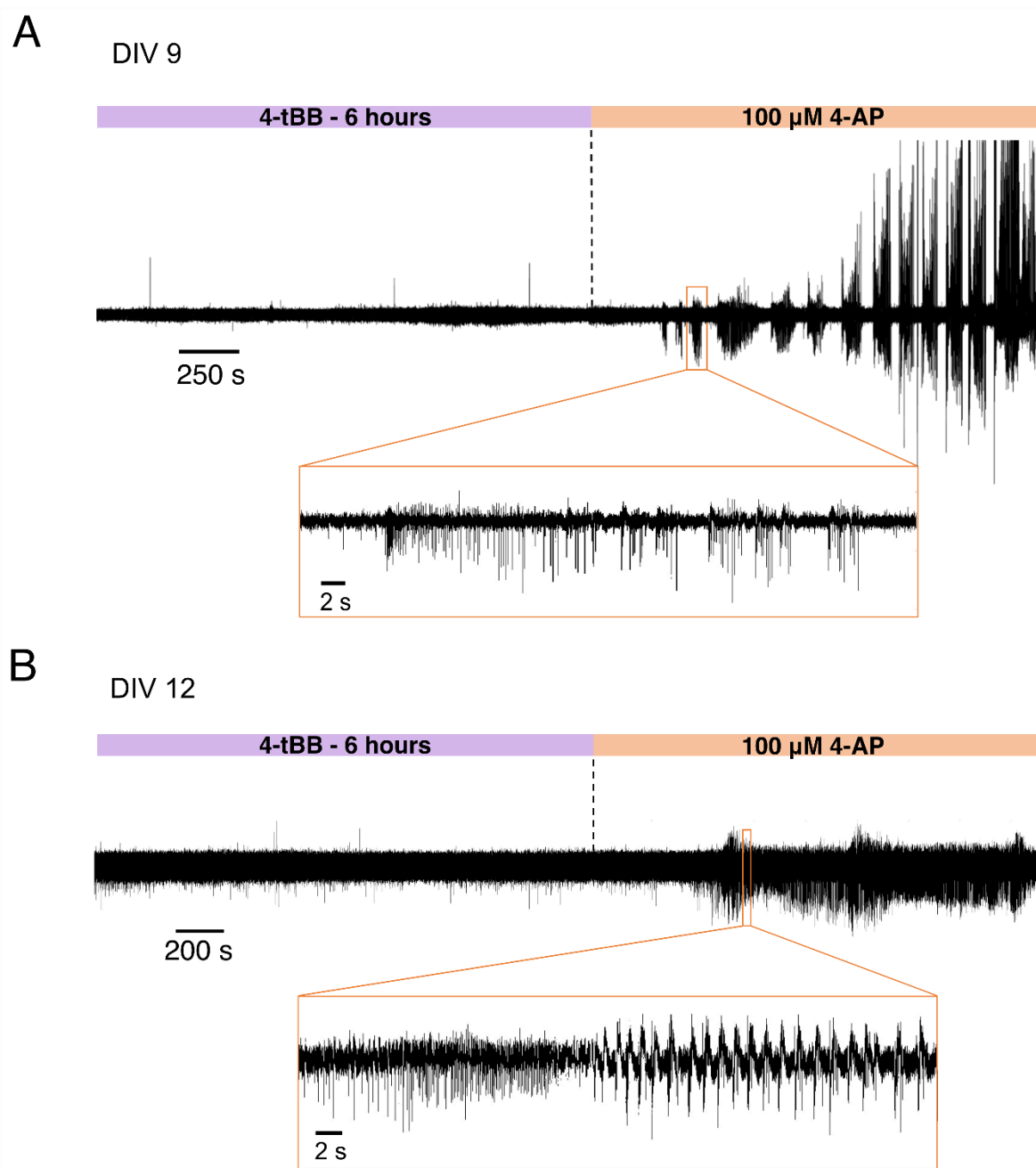
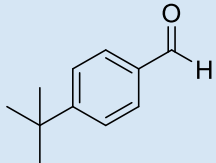
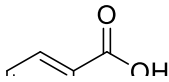
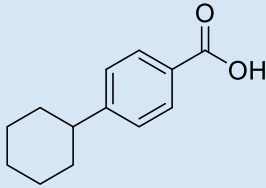
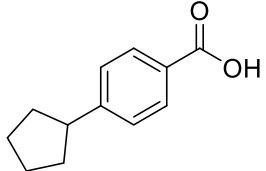
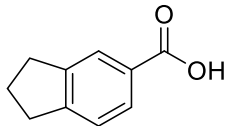
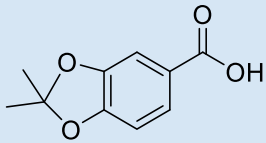
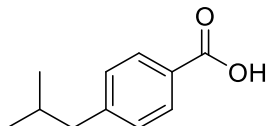
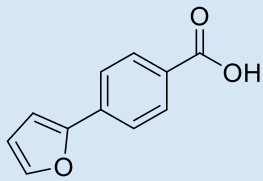
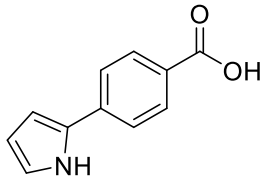
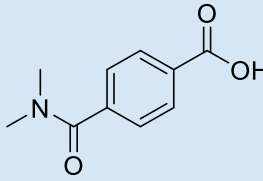
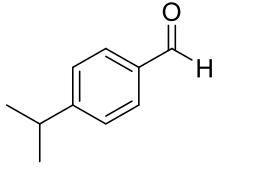
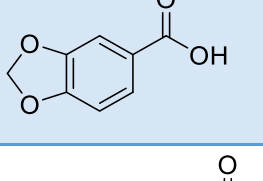
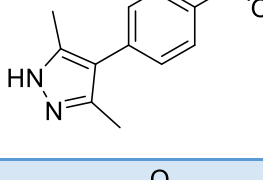
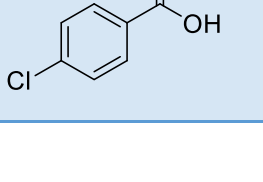


Fig. S1. Application of the K^+ channel blocker 4-aminopyridine (4-AP) shows that slices exposed to 4-TBB are healthy. The addition of 4-AP (100 μ M) to slices, following 6hrs exposure to 4-TBB (1.2mM), induces a rapid, and expected, increase in activity. Examples shown are from two independent slices where 4-AP triggered a reappearance of seizure-like activity that had been completely abolished by 4-TBB application.

Table S1. Structures and physicochemical properties of 4-TBB analogues screened for anticonvulsive activity in *Drosophila*.

Compound	Structure	MW (g/mol)	CLogP	Polar surface area Å ²	pKa	Synthesised / Purchased (source + cat no.)
4-TBB		162.23	3.49	17.07	N/A	FluoroChem: 065159
RAB201		247.99	3.12	37.30	3.8	Merck: ATC311764220
RAB202		204.11	4.51	37.30	4.3	Merck: AOBH961DC0B4
RAB204		190.09	3.95	37.30	4.3	Merck: AOBH97EBAF06
RAB205		290.01	3.56	37.30	3.0	Merck: ENA514506754
RAB206		162.06	2.90	37.30	4.1	Fluorochem: 059793
RAB207		194.05	2.61	55.76	3.9	Merck: COMH04239142
RAB208		178.09	-3.84	37.30	4.2	Fluorochem: 238558

RAB210		188.04	3.16	46.53	4.3	Fluorochem: 031925
RAB211		187.06	2.64	49.33	4.4	Synthesised
RAB212		193.07	0.61	57.61	4.2	Synthesised
RAB213		148.08	2.92	17.07	None	Fluorochem: 225406
RAB215		166.02	1.97	55.76	3.8	Fluorochem: 022643
RAB216		216.24	1.92	61.7	4.0	Synthesised
RAB217		156.57	2.70	37.3	4.0	Fluorochem: 118580